Extended Abstracts of the 22nd (1990 International) Conference on Solid State Devices and Materials, Sendai, 1990, pp. 39-42

B-1-7

Signal and Noise Modeling for Striped Channel Field-Effect Transistors

Yuji Ando, Masaaki Kuzuhara, Kazuhiko Onda,
Norihiko Samoto, and Tomohiro Itoh

Microelectronics Research Laboratories,
NEC Corporation, 4-1-1, Miyazaki, Miyamae-ku,
Kawasaki 213, JAPAN

The cylindrical metal-semiconductor field-effect transistor (MESFET) has been studied for modeling the two-dimensional charge-control behaviors in striped channel field-effect transistors (FETs). Modifying the classical approach presented by van der Ziel and Pucel *et al.*, the authors have developed the dc, small-signal, and noise model for cylindrical FETs. By using the present analysis, signal and noise properties for cylindrical FETs have been calculated and compared with the results for conventional FETs. Experimentally observed enhancement in charge- controllability is explained. Concerning noise properties, cylindrical FETs are shown to be equivalent to conventional FETs if transport properties are assumed to be identical. The striped channel FET is, however, considered to have a great potential as an ultra low-noise amplifier for microwave and millimeter-wave frequencies due to the reduced short channel effects as well as superior transport properties for quasi-one-dimensional (Q1D) electrons.

I. Introduction

With the resent progress in lithography and crystal growth techniques, there have been considerable reports on examining electron transport properties in quasi-one-dimensional (Q1D) semiconductor wires[1)-5)]. One of interesting approachs is the striped channel field-effect transistor (FET), which has parallel stripes of very narrow channels. Excellent dc and microwave performance for striped channel FETs has been demonstrated by Onda *et al.* [6)] and Kawasaki *et al.* [7)] . The striped channel FET has some attractive features:

1) Superior electron transports due to Q1D confinement;
2) improved charge-controllability; and
3) reduced short channel effects.

Transport properties for Q1D electrons have been studied by several authors [8)-10)]. There have been, however, no adequate model for explaining operation of striped channel FETs. Two-dimensional (2D) charge control behaviors make it difficult to understand the operation of striped channel FETs. The aim of this paper is to propose a dc, small-signal, and noise model for striped channel FETs including the 2D charge control characteristics. According to Rensch's approach[1)], the cylindrical metal-semiconductor FET (MESFET) will be studied for modeling striped channel FETs.

II. DC Conditions for Cylindrical FETs

Figure 1 illustrates geometries for the striped channel FET and cylindrical MESFET. The cylindrical MESFET consists of a cylindrical rod of conducting material with a radius a which is surrounded by a circular gate with a length L_g. Following Pucel *et al.* [11)], the channel is divided into two regions. Ohm's law applies for region I, while in region II, electrons travel with their saturation velocity v_s. According to the boundary conditions for Poisson's equation, cylindrical coordinates (r, ϕ, x) are introduced. The applied gate voltage V_{gs} modulates the thickness of a depletion layer ($a - b(x)$) and hence the radius of an active channel $b(x)$.

The gradual channel region (region I) for a cylindrical FET is analyzed based on the following assumptions:

1) The drift velocity v rises linearly with fields E_x ($< E_s$);
2) the longitudinal electric fields are negligible compared to the transverse fields (E_r), i.e., $E_x \ll E_r$; and
3) donors in the depletion layer are fully ionized.

Poisson's equation for the potential Ψ_1 in region I is

$$\begin{cases} \dfrac{1}{r}\dfrac{\partial}{\partial r}(r\dfrac{\partial}{\partial r}\Psi_1) = -\dfrac{qN_d}{\epsilon} & \text{for } b(x) \leq r \leq a \quad (1a) \\ \Psi_1(r,x) = V(x) & \text{for } 0 \leq r \leq b(x) \quad (1b) \\ \Psi_1(a,x) = V_{gs} - V_{bi} & (1c) \\ \dfrac{\partial \Psi_1}{\partial r}(b,x) = 0 & (1d) \end{cases}$$

where N_d is donor concentration, ϵ permittivity, V_{gs} the gate-source voltage, V_{bi} the built-in voltage for the Schottky barrier,

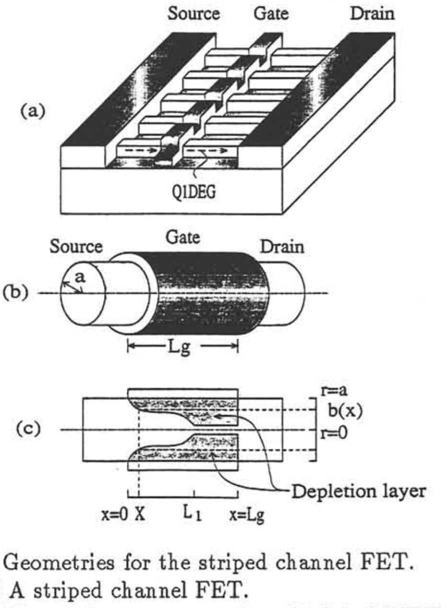

Fig. 1. Geometries for the striped channel FET.
(a) A striped channel FET.
(b) External appearance of a cylindrical MESFET.
(c) Cross-sectional view of a cylindrical MESFET.

and $V(x)$ the channel potential at a point x. To simplify the analysis, normalized radii for the active channel are introduced.

$$s = \frac{b(0)}{a},\ w = \frac{b(x)}{a},\ p = \frac{b(L_1)}{a}. \qquad (2)$$

From (1a)-(1d), $V(x)$ is obtained in terms of w.

$$V(x) - V_{gs} + V_{bi} = V_{po}(\frac{1-w^2}{2} + w^2 \ln w) \qquad (3)$$

where $V_{po} = qN_d a^2/(2\epsilon)$. From (3), the threshold voltage is

$$V_{th} = V_{bi} - \frac{V_{po}}{2}. \qquad (4)$$

Starting with the usual equations, one obtains drain current, length of region I, and the voltage drop for region I as

$$I_d = I_s p^2, \qquad (5)$$

$$L_1 = \frac{2V_{po}}{E_s p^2} H(4) \equiv L_g - L_2, \qquad (6)$$

and $\Delta V_1 = 2V_{po} H(2)$ (7)
respectively, where $I_s = qN_d \pi a^2 v_s$ and

$$H(n) \equiv \begin{cases} \frac{1}{n}\{p^n(\ln p - \frac{1}{n}) - s^n(\ln s - \frac{1}{n})\} & \text{for } n = 1, 2, 3, \cdots \\ \frac{1}{2}\{(\ln p)^2 - (\ln s)^2\} & \text{for } n = 0. \end{cases} \qquad (8)$$

The potential for the velocity saturation region (region II) is expressed by the sum of a particular solution for Poisson's equation and a homogeneous solution $\Psi_2(r, x)$. The Laplace's equation for Ψ_2 is

$$\begin{cases} \{\frac{\partial^2}{\partial r^2} + \frac{1}{r}\frac{\partial}{\partial r} + \frac{\partial^2}{\partial x^2}\}\Psi_2(r, x) = 0 & (9a) \\ \Psi_2(r, L_1) = 0 & (9b) \\ \Psi_2(a, x) = 0 & (9c) \\ \frac{\partial \Psi_2}{\partial x}(0, L_1) = -E_s. & (9d) \end{cases}$$

The solution for above equations are approximated by

$$\Psi_2(r, x) \approx -\frac{aE_s}{\rho_{01}} \sinh\{\frac{\rho_{01}(x - L_1)}{a}\} J_0(\frac{\rho_{01} r}{a}) \qquad (10)$$

where J_0 is the Bessel function of order 0 and $\rho_{01} \approx 2.4048$ is a minimum value for positive roots of $J_0(\rho) = 0$. Therefore, the channel voltage drop ΔV_2 through region II is

$$\Delta V_2 = \frac{aE_s}{\rho_{01}} \sinh(\frac{\rho_{01} L_2}{a}). \qquad (11)$$

From comparison between (11) and the Grebene - Ghandhi formulation[12]), it is shown that the channel potential varies more rapidly in cylindrical FETs than in conventional FETs. Summing (7) and (11), one obtains the drain voltage V_{ds}.

III. Small-Signal Parameters for Cylindrical FETs

From the analyses given in 13), we obtain the expressions for transconductance:

$$g_m = 4\pi\epsilon v_s f_g, \qquad (12)$$

drain output resistance:

$$r_d = \frac{f_r}{4\pi\epsilon v_s}, \qquad (13)$$

and gate-source capacitance:

$$C_{gs} = \frac{I_s}{\mu_0 E_s^2}(f_{c1} + f_{c2}), \qquad (14)$$

where $f_g = \frac{1}{f_r}\{(\frac{s}{p})^2 \cosh(\frac{\rho_{01} L_2}{a}) - 1\}$, (15)

$$f_r = 2\ln p - \{\ln p + \frac{1}{4} + (\frac{s}{p})^4(\ln s - \frac{1}{4})\}\cosh(\frac{\rho_{01} L_2}{a}), \qquad (16)$$

$$f_{c1} = \frac{s^2}{p^6}\{2\frac{p^6 \ln p - 2H(6)}{f_r}\cosh(\frac{\rho_{01} L_2}{a}) + p^4 s^2\}, \qquad (17a)$$

and $f_{c2} = s^2\{\frac{2}{f_r}(\frac{E_s L_g}{p^2 V_{po}} - \ln p)\cosh(\frac{\rho_{01} L_2}{a}) - 1\}$. (17b)

According to the preceding analysis, striped (cylindrical) channel FETs and conventional GaAs FETs are analyzed. For both structures, identical transport parameters ($\mu_0 = 4000 cm^2/\text{Vs}$ and $v_s = 1.2 \times 10^7$cm/s) are used. Figure 2 presents normalized transconductance (g_m/I_d) as a function of V_{gs} for cylindrical and conventional GaAs MESFETs. An enhancement in charge-controllability is expected for cylindrical FETs. This result qualitatively agrees with experimental findings reported by Onda *et al.* [6]). Figure 3 illustrates the unity current gain cutoff frequency (f_t) evolution versus I_d for a striped channel FET consisting of N cylindrical channels (raius a) and for a conventional GaAs FET with an equivalent channel width ($Z_g = 2Na$). Concerning f_t, these devices are equivalent as far as transport parameters are identical.

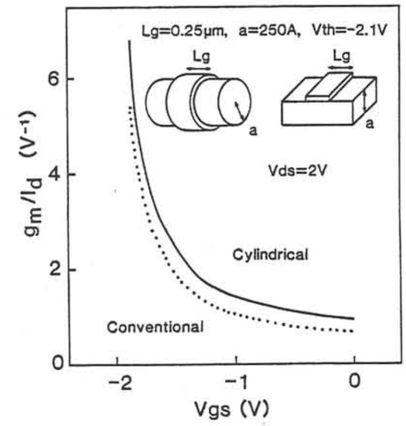

Fig. 2. Normalized transconductance (g_m/I_d) as a function of V_{gs} for cylindrical (solid line) and conventional (dotted line) GaAs FETs ($L_g = 0.25\mu$m, $a = 250\AA$, and V_{th}=-2.1V).

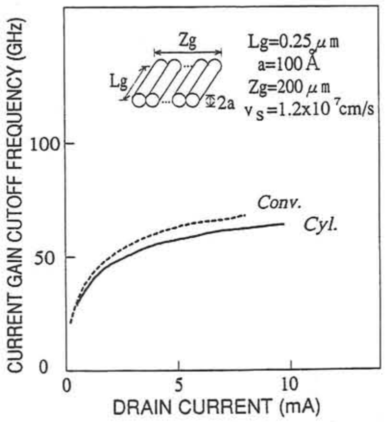

Fig. 3. Evolution of f_t versus I_d for striped channel FETs (solid line) consisting of 10000 cylindrical channels and conventional (dotted line) FETs with an equivalent gate width (Z_g = 200μm) (L_g = 0.25μm, a = 100$\AA$, and V_{th}=-2.1V).

IV. Noise Source Model for Cylindrical FETs

The noise model for cylindrical FETs was developed by modifying the earlier work by van der Ziel[14),15)], Statz-Haus-Pucel[11)] to a cylindrical FET version. The noise source is divided in two parts, i.e., Johnson noise from region I and high-field diffusion noise from region II. Only the final results will be written here. Details of analyses are given in 13).

The drain voltage fluctuation $\overline{v_{d1}^2}$ caused by the Johnson noise is calculated based on the following assumptions[11),14)]:
1) Gradual channel approximation holds;
2) the elementary noise voltage at a small segment ($x_0 < x < x_0 + dx_0$) in region I is described by the Nyquist formula:

$$\overline{\Delta v_x^2} = \frac{4kT_n \Delta f \Delta v_x}{I_d} \qquad (18)$$

where Δf is the frequency range, k the Boltzmann constant, and T_n the effective noise temperature; and
3) the intervalley scattering effects are included based on a simple expression for T_n presented by Baechtold [16)]:

$$T_n \approx T_0\{1 + \delta(\frac{E_x}{E_s})^3\} = T_0\{1 + \delta(\frac{p}{w})^6\}. \qquad (19)$$

where T_0 is the lattice temperature and δ is an empirical parameter.
The drain voltage fluctuation $\overline{\Delta v_{d1}^2}$ due to an elementary noise produced at x is obtained under ac open-circuit drain conditions. Summing $\overline{\Delta v_{d1}^2}$ over region I, $\overline{v_{d1}^2}$ can be calculated as

$$\overline{v_{d1}^2} = \frac{8kT_0 \Delta f V_{po}}{I_d} \cosh^2(\frac{\rho_{01} L_2}{a})[P_0 + P_\delta] \qquad (20)$$

$$\text{with} \quad P_0 = \frac{1}{p^4} H(6) \quad (21a) \qquad P_\delta = \delta p^2 H(0). \quad (21b)$$

At high frequencies, there are induced noise currents on the gate which is capacitively coupled to the channel. The induced gate charge Δq_1 due to an elementary noise produced at x_0 is obtained with ac short-circuit drain conditions[11),15)]. The induced gate currents can be derived by summing $\overline{\Delta i_{g1}^2} = \omega^2 \overline{\Delta q_1^2}$ over region I. The final expression can be written as

$$\overline{i_{g1}^2} = \frac{8kT_0 \Delta f V_{po}}{I_d} (\frac{2\omega L_1}{v_s p^2 r_d})^2 \cosh^2(\frac{\rho_{01} L_2}{a})[R_0 + R_\delta] \qquad (22)$$

$$\text{with} \quad R_0 = \frac{1}{p^4}\{\kappa'^2 H(6) + \kappa' \gamma H(8) + \frac{\gamma^2}{4} H(10)\} \qquad (23a)$$

$$\text{and} \quad R_\delta = \delta p^2 \{\kappa'^2 H(0) + \kappa' \gamma H(2) + \frac{\gamma^2}{4} H(4)\}, \qquad (23b)$$

$$\text{where} \quad \gamma = \frac{I_d r_d}{E_s L_1 \cosh(\frac{\rho_{01} L_2}{a})} \qquad (24)$$

$$\kappa' = \frac{1}{4H(4)}\{H(6) - \frac{p^6 - s^6}{24} - \frac{s^4}{2}(\ln s - \frac{1}{4})(p^2 - s^2)\} + \frac{p^2}{2}(\frac{L_2}{L_1} - \gamma). \qquad (25)$$

The diffusion noise from region II is interpreted as the shot noise due to traveling dipole layers[11)] generated at the rate

$$r_{dp} = \frac{2D_x n A}{\Delta x} \qquad (26)$$

where Δx and A are thickness and cross-section for dipole layers, respectively, D_x is the diffusion coefficient, and n is the carrier density. In the Statz model, D_x was assumed to be constant. However, the Monte-Carlo calculations indicate that D_x strongly depends on electric fields[17)]. Modifying the Einstein relation, we approximate the D_x variation versus $E_x (\geq E_s)$ by

$$D_x \approx D_h + \frac{kT_0}{q} \frac{v_s}{E_x} \qquad (27)$$

where D_h is the high-field diffusion coefficient[18)]. Using (27), we calculate the drain voltage fluctuation $\overline{v_{d2}^2}$ due to the diffusion noise. The final results are

$$\overline{v_{d2}^2} = \frac{2qaI_d \Delta f J_1(p\rho_{01})^2}{\pi^2 \epsilon^2 b_p^2 v_s^3 \rho_{01}^5 J_1(\rho_{01})^4}[D + \tilde{D}] \qquad (28)$$

$$\text{with} \quad D = D_h(3 + 2\ln\lambda + \lambda^2 - 4\lambda) \qquad (29a)$$

$$\tilde{D} = \frac{4kT_0 \mu_0}{q}\{\lambda(\lambda - 1) - \lambda \ln \frac{2\lambda^2}{1 + \lambda^2} - (\lambda^2 - 1)(\frac{\pi}{4} - \arctan\frac{1}{\lambda})\} \qquad (29b)$$

where $\lambda = \exp(\frac{\rho_{01} L_2}{a})$ and $b_p = ap$.

Modifying the Statz-Haus-Pucel model [11)], the diffusion noise induced gate currents are calculated, as is seen by

$$\overline{i_{g2}^2} = \frac{8qI_d \Delta f a L_1^2 \omega^2 \kappa'(\gamma = 0)^2 J_1(p\rho_{01})^2}{\pi^2 \epsilon^2 b_p^2 r_d^2 v_s^5 p^4 \rho_{01}^5 J_1(\rho_{01})^4}[D + \tilde{D}]. \qquad (30)$$

The gate and drain noise currents are correlated since they originate both from the thermal noise in channel. Fluctuating fields and potentials modulate the carrier velocity as well as the depletion layer thickness. Since the velocity change gives no contribution to gate currents, the correlation coefficient (C_{11}) between i_{g1} and i_{d1} becomes so much smaller than unity.

$$C_{11} \equiv \frac{\overline{i_{g1}^* i_{d1}}}{j\sqrt{\overline{i_{g1}^2} \cdot \overline{i_{d1}^2}}} = \frac{S_0 + S_\delta}{\sqrt{[P_0 + P_\delta][R_0 + R_\delta]}} \qquad (31)$$

$$\text{with} \quad S_0 = \frac{1}{p^4}\{\frac{\gamma}{2} H(8) + \kappa' H(6)\} \qquad (32a)$$

$$\text{and} \quad S_\delta = \delta p^2 \{\frac{\gamma}{2} H(2) + \kappa' H(0)\}. \qquad (32b)$$

Since the noise in region II causes no velocity change, there is a full correlation between i_{d2} and i_{g2}. Therefore their correlation coefficient is

$$C_{22} = 1. \qquad (33)$$

V. Noise Properties for Striped Channel FETs

The minimum noise figure F_{min} is given in terms of small-signal parameters, drain noise coefficient P, gate noise coefficient R, and correlation coefficient C [11),18)], which are easily calculated according to the preceding analysis. Noise properties for striped channel FETs are studied and compared to the conventional GaAs FETs with an equivalent channel width. Typical parameters used for calculations are V_{bi}=0.8V, ϵ/ϵ_0=12.5, δ=2, μ_0=4000cm^2/Vs, $v_s = 1.2 \times 10^7$cm/s, and D_h=35cm^2/s. Identical parameters are assumed for both FETs.

Noise coefficients are calculated for striped channel and conventional FETs. Concerning P, R, and C at optimum I_d, no important superiority is expected for striped channel FETs. Figure 4 illustrates F_{min} dependence on I_d. The striped channel FET shows a comparatively flat dependence of F_{min} on bias conditions. Regarding optimum F_{min} values, these devices are equivalent. These results explain the experimental findings reported by Kawasaki *et al.* [7)]. The F_{min} evolution versus frequency is shown in Fig. 5.

So far, striped channel FETs have been compared to conventional FETs with identical parameters. Figure 6 illustrates the influence of saturation velocity on F_{min}. It is shown that superior transports of Q1D channels dramatically improve noise characteristics for striped channel FETs.

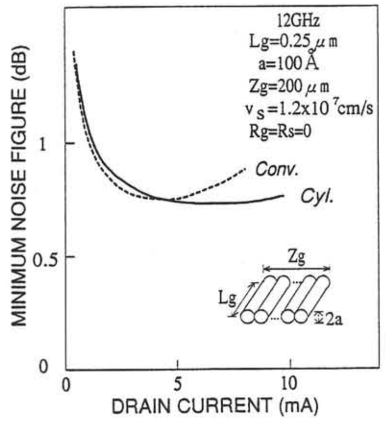

Fig. 4. Evolution of F_{min} (12GHz) versus I_d for cylindrical (solid line) and conventional (dotted line) FETs with $R_g = R_s$=0. Other device parameters are the same as those for Fig. 3.

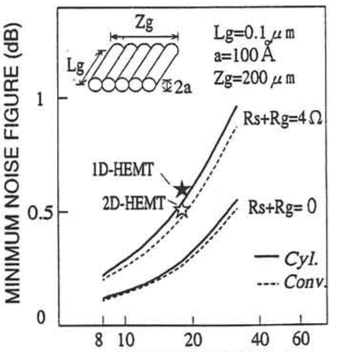

Fig. 5. F_{min} dependence on frequency for a striped channel FET (solid lines) consisting of 10000 cylindrical channels and for a conventional FET (dotted line) with an equivalent gate width (Z_g=200μm) (L_g = 0.1μm, a = 100Å, V_{th}=-2.1V, and $R_s + R_g$=0 and 4Ω). ★ and ☆ denote experimental data for striped and conventional HEMTs, respectively [7].

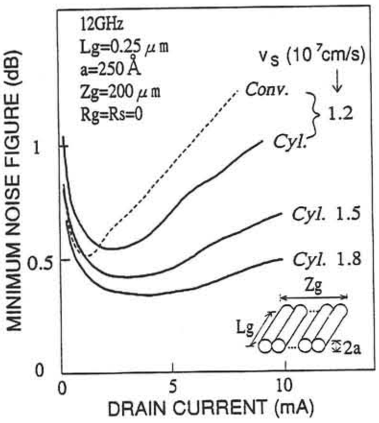

Fig. 6. Evolution of F_{min} (12GHz) versus I_d for a striped channel FET (solid lines) consisting of 4000 cylindrical channels and for a conventional FET (dotted line) with an equivalent gate width (Z_g=200μm) (L_g = 0.25μm, a = 250Å, and V_{th}=-2.1V). The v_s is ranged between 1.2 and 1.8 ×10^{7}cm/s. For a conventional FET, the result is shown only for v_s = 1.2 × 10^{7}cm/s.

VI. Conclusion

In summary, the cylindrical MESFET has been studied for modeling the 2D charge-control behaviors in striped channel FETs. The authors have developed the dc, small-signal, and noise model for cylindrical FETs. By means of the present theory, signal and noise properties for striped channel FETs have been analyzed. Features for noise properties of striped channel FETs are

1) Supposing transport properties are identical, striped and conventional FETs are equivalent concerning optimum F_{min};
2) a high f_t due to superior transport properties of Q1D electrons improves the noise performance; and
3) suppressed short channel effects allow for reducing L_g without suffering from an increase in the drain noise.

Consequently, the striped channel FET is considered to have a great potential to be a low-noise amplifier for microwave and millimeter-wave frequencies.

Acknowledgment

The authors would like to thank K.Nakamura and F.Nihey for meaningful discussions and help. They would like to thank H.Sakuma and T.Nozaki for their encouragement.

References

1) D.B.Rensch *et al.* ; *IEEE Trans.Electron Devices* ED-34 (1987) 2232.
2) K.Ismail *et al.* ; *J.Vac.Sci.Technol.B* 6 (1988) 1824.
3) M.Okada *et al.* ; *Jpn.J.Appl.Phys.* 27 (1988) L2424.
4) K.Tsubaki *et al.* ; *Electron.Lett.* 24 (1988) 1267.
5) R.C.Clarke; *Proc.IEEE/Cornell Conf.* (New York 1983) 83.
6) K.Onda *et al.*; *Proc.1989 IEDM* (Washington,D.C. 1989) 125.
7) H.Kawasaki *et al.* ; presented at *the 37th Spring Meeting of the Japan Society of Applied Physics and Related Societies*(Asaka 1990).
8) H.Sakaki; *Jpn.J.Appl.Phys.*19 (1980) L735.
9) J.P.Leburton; *J.Appl.Phys.*56 (1984) 2850.
10) T.Yamada and J.Sone; *Proc.ICEM* (Tokyo 1988) 96.
11) R.A.Pucel *et al.* ; *Advanced Electron.Electron Phys.* 38 (1974) 195.
12) A.B.Grebene and S.K.Ghandhi; *Solid-State Electron.*12 (1969) 573.
13) Y.Ando *et al.* ; submitted to *IEEE Trans.Electron Devices.*
14) A.van der Ziel; *Proc.IRE* 50 (1962) 1808.
15) A.van der Ziel; *Proc.IEEE* 51 (1963) 461.
16) W.Baechtold; *IEEE Trans.Electron Devices* ED-19 (1972) 674.
17) Y.Ando and T.Itoh; *IEEE Trans.ElectronDevices* 37 (1990) 67.
18) A.Cappy; *IEEE Trans.Microwave Theory Tech.* 36 (1988) 1.